

Advances of high-birefringence fiber loop mirror sensors

YONG ZHAO*, HONGKE WU, QI WANG

Northeastern University, College of Information Science and Engineering, Shenyang 110004, China

High-Birefringence fiber loop mirror(Hi-Bi FLM) sensor has been one of the hot issues in optical fiber sensor technologies. This paper introduced the fundamental principle of Hi-Bi FLM and also characterized the temperature and strain features of conventional and photonic crystal Hi-Bi FLM. Furthermore, we selectively enumerated various simultaneous measurements of temperature and strain based on Hi-Bi FLM, and the distinguishes between them were particularly analyzed. These measurements not only avoided the problems of cross-sensitive but also expanded the Hi-Bi FLM application fields.

(Received April 7, 2011; accepted May 25, 2011)

Keywords: High-Birefringence, Fiber loop mirror, Photonic crystal fiber, Temperature sensor, Strain sensor

1. Introduction

As a new-style optical interferometric component, FLM has been applied in many fields due to its advantages such as high anti-interference, high sensitivity and simple structure. Recently, a section of high-birefringence fiber(HBF) is cascaded into FLM, so Hi-Bi FLM is formed. Compared with traditional FLM, Hi-Bi FLM has many advantages: (1) Polarization independence.(2) Transmission spectra is only concerned with the length of HBF, but not the diameter of Hi-Bi FLM. Based on these advantages above, Hi-Bi FLM has been widely used in optical wavelength division, tunable laser and comb filter [1-3].

In recent years, more and more attentions are paid to Hi-Bi FLM sensor. It has been used not only in strain and temperature measurements [4], but also in liquid level[5] and curvature [6] measurements.FBG sensor was also demodulated by Hi-Bi FLM[7]. But it is easily influenced by temperature when using the traditional polarization-maintaining fiber(PMF) as the sensing element. So we must eradicate the cross-sensitive of traditional polarization- maintaining fiber when it is used as sensor. Two methods are taken to avoid this problem, for one thing, as the high-birefringence photonic crystal fiber(Hi-Bi PCF[8])which were immune to temperature generated, we can choose Hi-Bi PCF as sensing element to avoid temperature effect. For another thing, several simultaneous measurements of temperature and strain based on Hi-Bi FLM were proposed to avoid cross-sensitive, this not only avoid cross-sensitive of Hi-Bi FLM sensor but also expanded the application fields of Hi-Bi FLM sensor.

This paper introduced fundamental principle of Hi-Bi FLM sensor firstly, then summarized and compared the temperature and strain characteristics of HBF including traditional and photonic crystal fiber reported

previously,also,listed six kinds of simultaneous measurement of temperature and strain based on Hi-Bi FLM .Last, we lookout the perspective of Hi-Bi FLM sensor.

2. Temperature and strain characteristics of Hi-Bi FLMs

As shown in Fig.1, the configuration consists of an optical broadband source(BBS) with a central wavelength of 1550 nm and a spectral bandwidth of 100 nm, an FLM containing a section of high-birefringence fiber(HBF),a PC and a optical spectrum analyzers(OSA).All these optical instruments are linked by single optical fiber (SMF-28). HBF is spliced with single optical fiber by welding machine, making the insertion loss is less than 4dB/km.

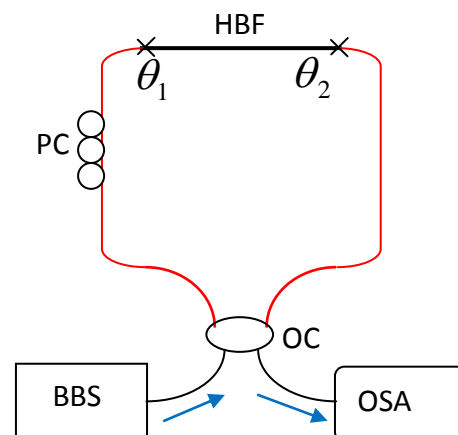


Fig.1. Structure of Hi-Bi FLM.

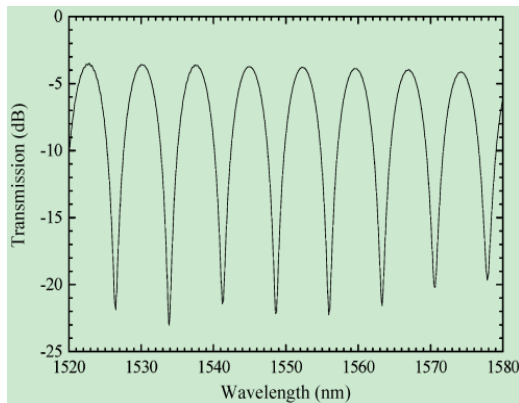


Fig. 2. Transmission spectra of Hi-Bi FLM

Broadband source(BBS) launches the light into 3dB coupler which splits the light into two counter propagating beams, then the two beams bring about phase difference when propagating through the HBF. The counter propagating beams recombine at the 3dB coupler and interference due to the phase difference. The relationship [9] between transmission spectrum and wavelength is as follows:

$$T(\lambda) = \left\{ \sin(\theta_1 + \theta_2) \cos \left[\frac{\pi L(n_e - n_o)}{\lambda} \right] \right\}^2 \quad (1)$$

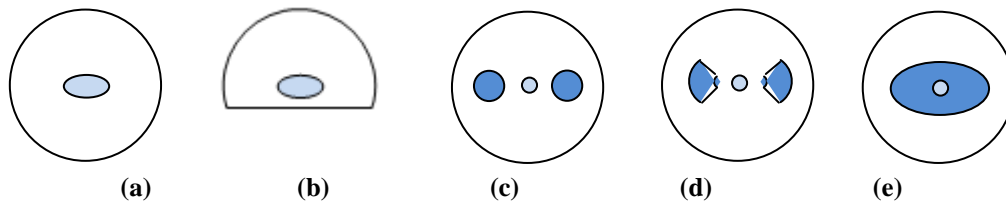


Fig. 3. Cross section of HBF a) elliptical core b) half-cladding fiber(D-type) c) panda d) bow-tie e) internal elliptical clad fiber(IEC)

Table.1 presented all the polarization-maintaining fibers [11]:

Table1 summarizing polarization-maintaining fibers

Fiber types	Birefringence (10 ⁻⁴)	Beat length (mm)	Insertion loss (dB/km)	Company
panda	3.85	4.0	9	KVH
bow-tie	4.71	3.3	9	KVH
IEC	3.3	4.65	1	Thorlabs
elliptical core	4.35	3.56	2	Fibercore
D-type	5.1	3.0	1	3M

where θ_1 、 θ_2 are the angles between fast axis of HBF and two counter propagating beams light respectively. Different light intensity of transmission spectrum is obtained with different θ_1 、 θ_2 which can be adjusted by PC. B is considered as initial birefringence of HBF which is expressed as $B = |n_e - n_o|$, where n_e 、 n_o are the effective refractive index of fast axis and slow axis of HBF respectively. L is the length of HBF and λ is the center wavelength of the BBS.

2.1 Conventional Hi-Bi FLMs

As shown in Fig.3, polarization-maintaining fiber[10] is considered as the common HBF that include panda, bow-tie, internal elliptical clad (IEC), e-core and D-type. According to the theory of high- birefringence fiber, we divide the polarization-maintaining fibers into two types: geometric effect and stress effect HBF. Panda, bow-tie and internal elliptical clad fiber are considered as stress effect HBF just because the birefringence is caused by asymmetrical stress region. Similarly, e-core and D-type HBF are considered as geometric effect fiber just because the birefringence is caused by asymmetrical core.

Temperature and strain characteristics for five types of HBFs presented above are characterized in experimental setup shown in fig.4. The optical source is an Erbium-doped broadband source, with a central wavelength of 1550 nm and a spectral bandwidth of 100 nm. The Hi-Bi FLM is formed by a 3 dB coupler with low insertion loss, an optical polarization controller (PC) used to adjust polarization state of the lights, a section of HBF. The sensing head is attached to a translation stage with a resolution of 1μm and enclosed within an oven with an error of about 1°C. The resolution of OSA adopted is 0.01nm. Fig.5 and Fig.6 show temperature and strain characters of panda, bow-tie, internal elliptical clad(IEC) HBF respectively.

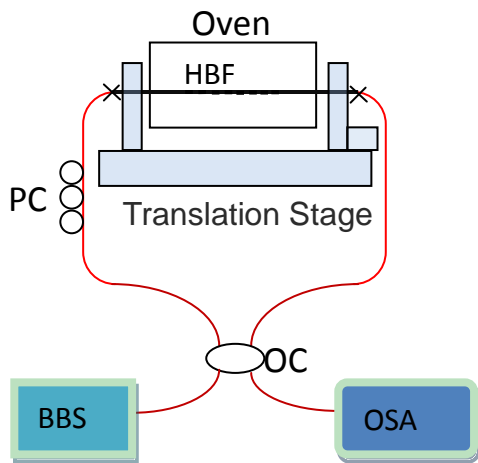


Fig. 4. Configuration of Hi-Bi FLM.

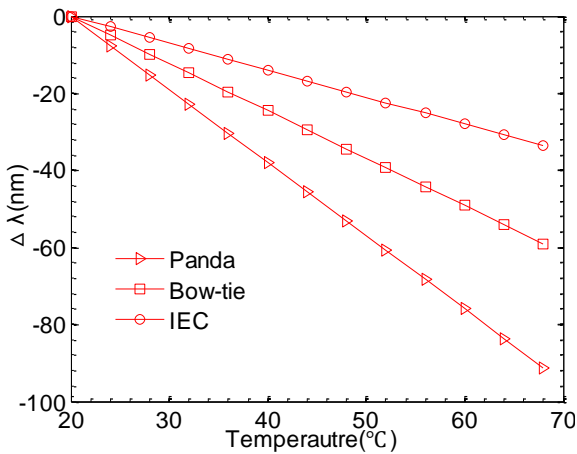


Fig. 5 Temperature characteristic.

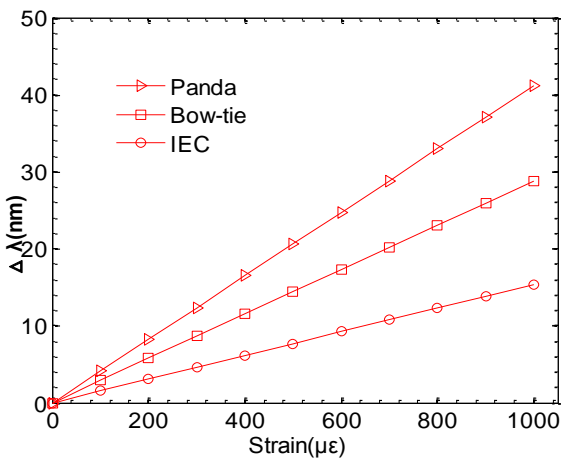


Fig.6 Strain characteristic.

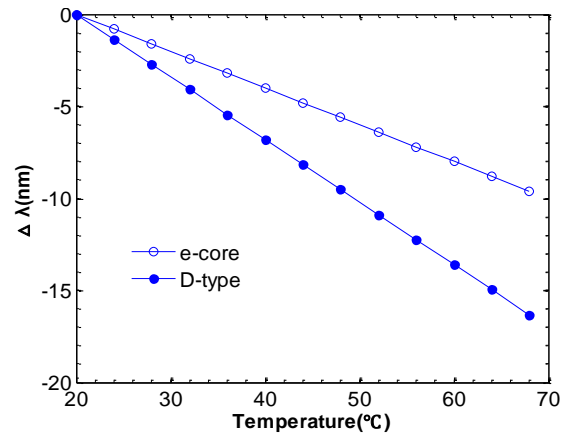


Fig. 7. Temperature characteristic.

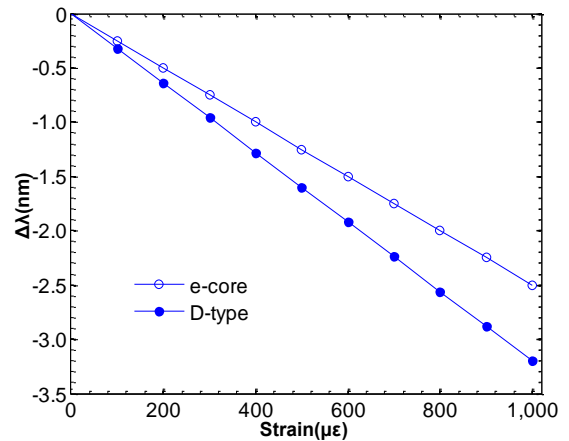


Fig. 8. Strain characteristic.

Temperature and strain characteristics of e-core and D-type HBF are also characterized in the same setup shown in Fig. 4. Compared with the foregoing three types of HBF, they have the lower sensitivities to temperature and strain, what's more, the sign of strain sensitivity is negative, as shown in fig.8 and fig.9. Sensitivities to temperature and strain of five types of HBF are shown in Table.2.

Table 2. Sensitivities to temperature and strain of five types of Hi-Bi FLMs.

Fiber types	strain(pm/μm)	temperature(nm/°C)
PADNA	41.2	-1.9
Bow-tie	28.8	-1.23
IEC	15.4	-0.7
e-core	-2.5	-0.2
D-type	-3.2	-0.34

2.2 Photonic crystal Hi-Bi FLMs

In recent years, special attentions are paid to photonic crystal fiber(PCF)[12] because of its merits including the property of single mode, high nonlinearity, high birefringence and controllable group velocity dispersion which conventional optical fiber don't have. PCF have an arrangement of microscopic air holes running along its length and by varying the size and location of the holes can reach values that are not achievable in conventional fiber. The below three types of Hi-Bi PCF are common ones that usually combined with fiber loop mirror, their cross sections are shown in Fig. 9.

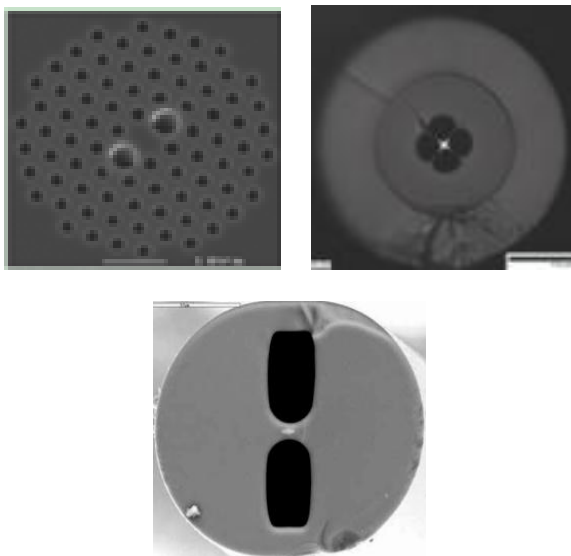


Fig. 9. a) panda Hi-Bi PCF; b) four-hole suspended core Hi-Bi PCF; c) side-hole Hi-Bi PCF.

A panda Hi-Bi PCF is the one of the acquainted Hi-Bi PCF, the meters of the holes are $4.5\mu\text{m}$ and $2.2\mu\text{m}$ respectively, the pitch (spacing between holes) is $4.4\mu\text{m}$, and the diameter of the perforated region is $40\mu\text{m}$, the whole outer diameter is $125\mu\text{m}$. Asymmetric defect in the core area is introduced to cause the high-birefringence effect. b) four-hole suspended core Hi-Bi PCF [13], the core and the cladding have diameters of $5.0\mu\text{m}$ and $135.0\mu\text{m}$ respectively. The core is slightly elliptical owing to the hole asymmetry originated fabrication process. The two types Hi-Bi PCFs are all made of pure silicium so they are immune to temperature. But if coated with acrylic acid, they will become sensitive to temperature[14] because the acrylic acid has the different thermal expansion coefficient with pure silicium. c) The side-hole Hi-Bi PCF [15] shown in fig.9 has a core dimension of $6.3 \times 2.5 \mu\text{m}$ (elliptical shape), a cladding of $125\mu\text{m}$, bridge between the holes is very narrow, so that the distance between the core edge and the holes edges does not exceed $2\text{--}3\mu\text{m}$. High-birefringence effect is induced by elliptical shape of the core and by mode overlap with the air holes

surrounding the core. A low loss splice (about 2 dB/km) [16-17] between single mode optical fiber and three types of Hi-Bi PCFs above is achieved to form Photonic crystal Hi-Bi FLMs. Temperature and strain characteristics of panda and four-hole suspended core PCF are characterized by the same configuration described in Fig.4. Their temperature and strain characteristic are shown in Fig.10, Fig.11, Fig.12, Fig.13 when they are coated or uncoated respectively.

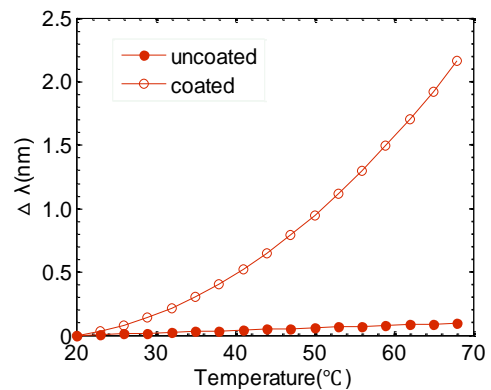


Fig.10. Temperature characteristic of panda

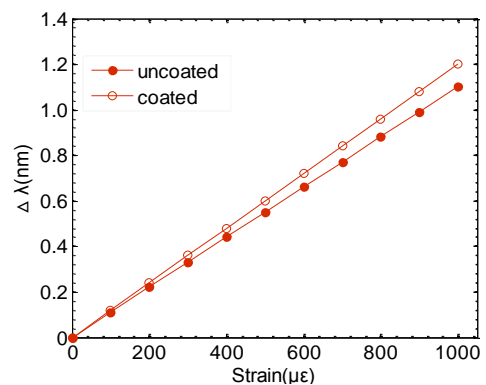


Fig.11. Strain characteristic of panda.

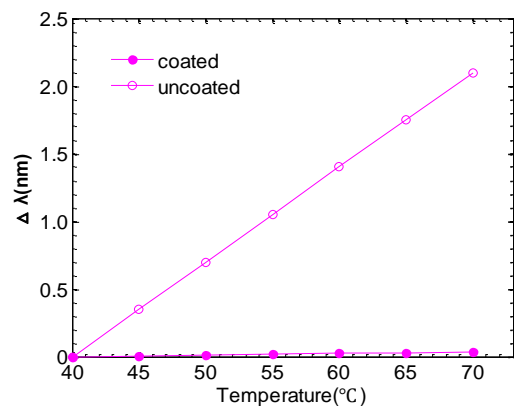


Fig.12 temperature characteristic of four-hole suspended core.

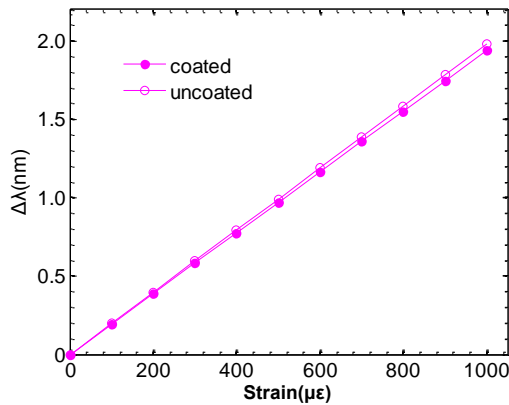


Fig.13 strain characteristic of four-hole suspended core

Using the same configuration described in Fig. 4, we all characterize the temperature and strain characters of side-hole Hi-Bi fiber experimentally. Fig.14 and Fig.15 presented its temperature and strain Characteristics.

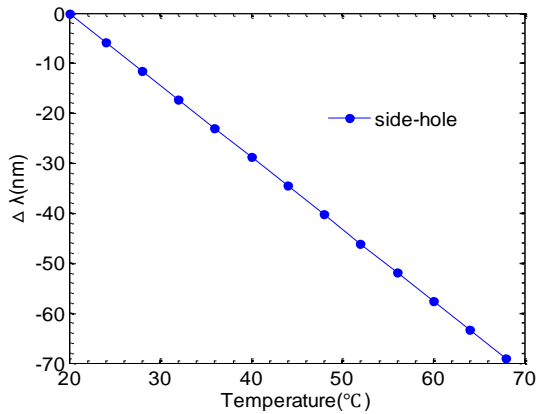


Fig.14 temperature characteristic of side-hole suspended core

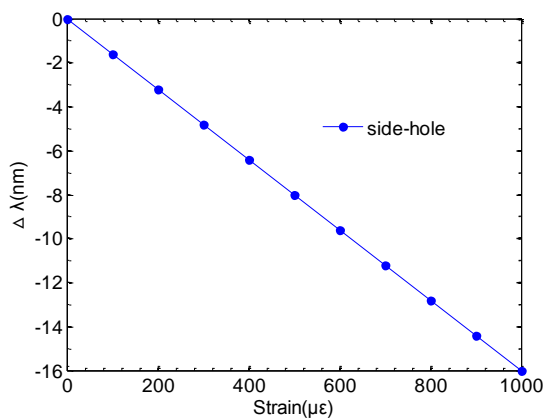


Fig.15 Strain characteristic of side-hole suspended core

Temperature and strain characteristics are listed in Table.3, as for the same Hi-Bi PCF, it has the higher sensitivity to temperature when it is coated, but almost the

same sensitivity to strain whether it is coated or not. Different Material for cladding and core are responsible for the intervallic sensitivity when they are coated or uncoated. Due to the special structure of side-hole Hi-Bi PCF, it has the more distinct sensitivities to temperature and strain than panda and suspended-core ones, about one or two order higher.

Table 3. Temperature and strain characteristics of three types of Hi-Bi PCF coated and uncoated.

Hi-Bi PCF types	Strain(pm/μm)	Temperature(nm/°C)
Panda uncoated	1.11	2.9×10^{-4}
Panda coated	1.12	0.9×10^{-2}
Suspended-core uncoated	1.93	3.4×10^{-4}
Suspended-core coated	1.94	7×10^{-2}
Side-hole	16	1.44

3. Measurements of dual parameters based on Hi-Bi FLM

As known from 2.1 and 2.2 chapters, Hi-Bi fibers including conventional and photonic crystal fiber are all sensitivity to temperature and strain simultaneously. So across- sensitivity exists when Hi-Bi FLM used as a sensor. In order to solve this problem, for one thing, we attempt to chose the uncoated Hi-Bi PCF which has almost to zero sensitivity to temperature as sensing element on the condition that it meet the need of external stress. For another thing, Hi-Bi FLM incorporating with other optical components realized simultaneous measurement of temperature and strain, this not only avoid the across-sensitivity for temperature and strain, but also expand the application of Bi-BI FLM.

3.1 A sensing element embedded in Hi-Bi FLM

Sensing element such as FBG, LPG or a section of another Hi-Bi fiber are embedded in Hi-Bi FLM to realize simultaneous measurement of temperature and strain.

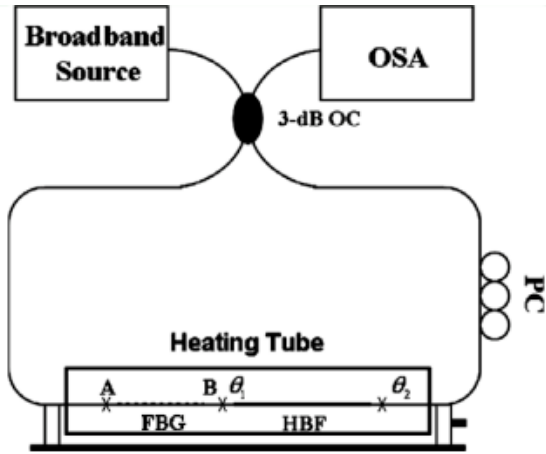


Fig.12 Hi-Bi FLM combined with FBG.

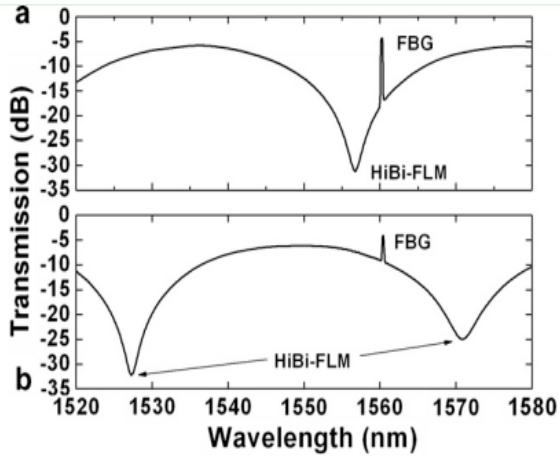


Fig.13 Transmission spectra at 22.3 °C and 40 °C respectively.

3.1.1 Fiber grating embedded in Hi-Bi FLM

As shown in Fig.12, Dapeng Zhou[18] proposed that a section of FBG was embedded in Hi-Bi FLM. FBG and Hi-Bi fiber were considered as sensing elements to realize simultaneous measurement of temperature and strain. Transmission spectra of Hi-Bi FLM and Bragg wavelength are monitored by OSA to determine the change of temperature and strain. In the experiment, initial Bragg wavelengths of FBG is 1560.05nm, with its reflectivity of 84.5%. We choose 12cm long bow-tie polarization maintaining optical fiber as Hi-Bi fiber with its initial birefringence of 4.55×10^{-4} at 1550nm. The whole transmission spectra is shown in fig.13 at 22.3 °C and 40 °C respectively.

As the temperature applied on the sensing head increased, the Bragg wavelength is redshifted, while the interferometric peaks of Hi-Bi FLM is blueshifted. As the

axial strain applied on the sensing head increased under invariable temperature, the Bragg wavelengths and interferometric peaks of FLM both redshifted. Thus Eq.2 was obtained as follows:

$$\begin{bmatrix} \Delta\lambda_{FBG} \\ \Delta\lambda_{HiBi-FLM} \end{bmatrix} = \begin{bmatrix} K_{T(FBG)} & K_{\varepsilon(FBG)} \\ K_{T(HiBi-FLM)} & K_{\varepsilon(HiBi-FLM)} \end{bmatrix} \begin{bmatrix} \Delta T \\ \Delta\varepsilon \end{bmatrix} \quad (2)$$

where ΔT and $\Delta\varepsilon$ are the temperature and strain change respectively. $K_{T(FBG)}$ 、 $K_{\varepsilon(FBG)}$ and $K_{T(HiBi-FLM)}$ 、

$K_{\varepsilon(HiBi-FLM)}$ are the corresponding temperature and strain coefficients which can be determined by experiment. When temperature and strain applied to the sensing head vary, Bragg wavelength and interferometric peak of FLM shift, thus a well-conditioned system of two equations can be written and expressed in a matrix:

$$\begin{bmatrix} \Delta T \\ \Delta\varepsilon \end{bmatrix} = \frac{1}{D} \begin{bmatrix} K_{\varepsilon(HiBi-FLM)} & -K_{\varepsilon(FBG)} \\ -K_{T(HiBi-FLM)} & K_{T(FBG)} \end{bmatrix} \begin{bmatrix} \Delta\lambda_{FBG} \\ \Delta\lambda_{HiBi-FLM} \end{bmatrix} \quad (3)$$

where $D = K_{T(FBG)} K_{\varepsilon(HiBi-FLM)} - K_{\varepsilon(FBG)} K_{T(HiBi-FLM)}$, measurand can be determined by monitoring the wavelengths shifts. Similar with the method reported in [18], O. Frazão[19] substituted FBG for a section of LPG to realize simultaneous measurements of temperature and strain alike.

3.1.2 Two sections of different Hi-Bi fibers embedded in Hi-Bi FLM

Guoyong Sun [20] reported two section of Hi-Bi fiber with different parameters are embedded in the FLM forming a novel Hi-Bi FLM. Due to the different sensitivities to temperature and strain, two wavelength dips can be monitored to realize simultaneous measurements of temperature and strain. In experiment, the lengths of two sections of Hi-Bi fiber are 4cm and 11cm with the birefringence 3.75×10^{-4} and 1.15×10^{-4} respectively. As shown in fig.14, the transmission spectra of novel fiber loop mirror.

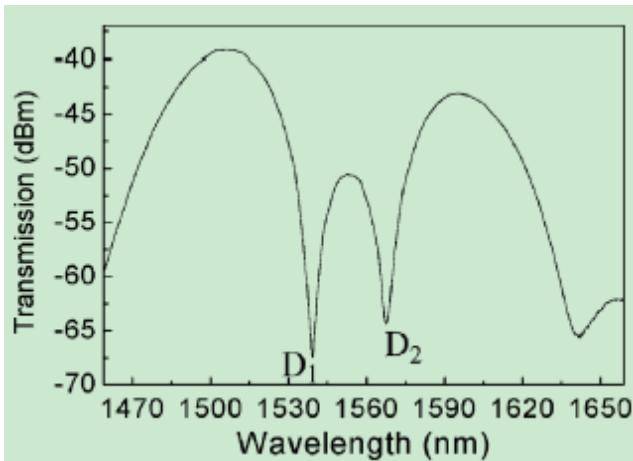


Fig.14 Transmission spectra of two-types HBF fiber loop mirror.

Those two types methods proposed above represented simultaneous measurements of temperature and strain based on Hi-Bi FLM. As for FBG, it is more easier and accurate to obtain shift of wavelength due to the narrower bandwidth of Bragg wavelength compared with LPG. Also, transmission spectra show high similarity between LPG and Hi-Bi FLM, We should adjust PC successively to get the proper transmission spectra. As for method in[20],perfect transmission spectra depends on the polarization state when they propagate through the two sections of Hi-Bi fiber, so we should try our best to keep the polarization state of the light.

3.2 External optical element combined with Hi-Bi FLM

3.2.1 Filtering Hi-Bi FLM by LPG

As shown in fig.16, Chun-Liu Zhao [21] reported a method based on Hi-Bi FLM combined with long period grating (LPG) inscribed in photonic crystal fiber for simultaneous measurement of strain and temperature. Here, the LPG in PCF acts as a temperature-insensitive optical wavelength filter which has a broad transmission dip and two spectral regions with opposite slopes shown in fig.17. Utilizing this property of the LPG, we choose two adjacent transmission peaks of the Hi-Bi FLM to be located at the two spectral regions. Transmission peaks shift were signed as $\Delta\lambda$, and two adjacent transmission peaks power are signed as P_1 、 P_2 respectively, dealing with $\Delta p = -\lg(p_1/p_2)$. When the temperature applied on the sensing head increases under invariable axial strain, the transmission peaks blueshift, $\Delta\lambda$ increased negatively and Δp decreased. When the axial strain applied on the sensing head increases under invariable temperature, the transmission peaks redshift, $\Delta\lambda$ increased positively and so Δp .by monitoring the $\Delta\lambda$

and Δp , we can distinguish temperature and strain simultaneously.

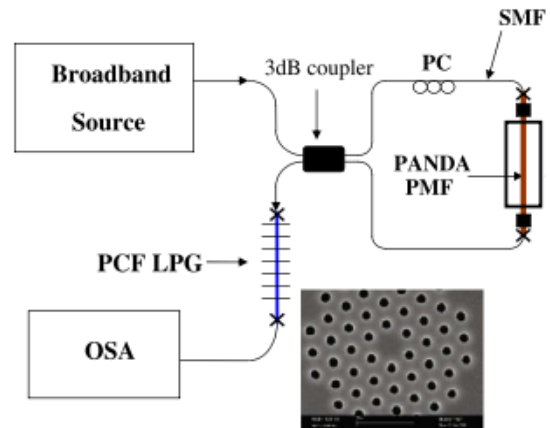


Fig.16 Hi-Bi FLM filtered by LPG.

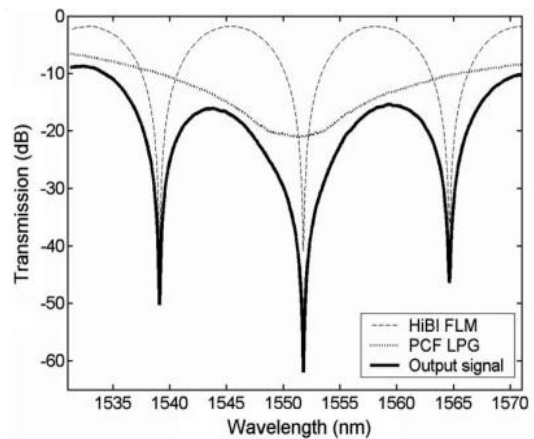


Fig.17 Transmission spectra of the FLM and of the LPG in PCF and the output signal.

3.2.2 Concatenated Hi-Bi FLMs

As shown in fig.18, O. Frazão [22] reported a resolution of simultaneous measurement of strain and temperature by using two concatenated Hi-Bi FLMs with one of the Hi-Bi FLMs containing Hi-Bi photonic crystal fiber(PCF) and another one containing conventional Hi-Bi fiber(internal elliptical cladding).Fig.19 presented the first and the concatenated Hi-Bi FLMs transmission spectra. The first Hi-Bi FLM emerged a proportionally large linear spectral region of about 17nm, then launched into the second Hi-Bi FLM through the opto-isolator which keep the light from flashbacking. Power of the transmission spectrum peaks of wavelength falling inside the linear spectral region is degressive. As the temperature applied on the sensing head increased under invariable axial strain, its peaks wavelength increased while power decreased. As the axial strain applied on the sensing head increased

under invariable temperature, peaks wavelength and power presented oppositely compared with temperature response. We can distinguish temperature and strain simultaneously by monitoring the power and wavelength of one of the peaks of the concatenated Hi-Bi FLMs.

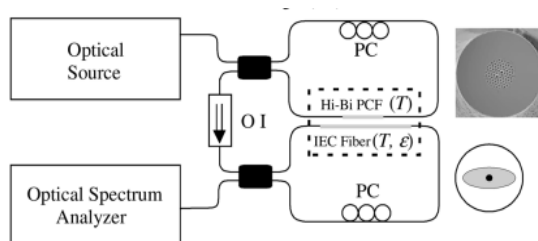


Fig. 18 structure chart of concatenated Hi-Bi FLMs.

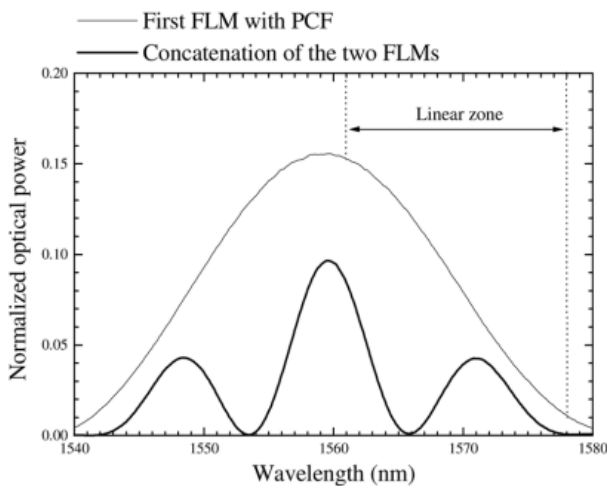


Fig. 19 Spectral responses of the first FLM and of the concatenated FLMs.

3.2.3 Hi-Bi FLM incorporating an Erbium-doped fibre (EDF)

As shown in fig.20, a section of erbium-doped fibre (EDF) joined into the input arm of Hi-Bi FLM [23]. When it was pumped, amplified spontaneous emission (ASE) light was generated which was also the light source of the whole configuration. The transmission spectrum peak power of the Hi-Bi FLM was reduced as the temperature increased because the amplified spontaneous emission (ASE) of the pumped EDF was degraded with the temperature increasing. So the temperature affected both the peak power and the peak wavelength simultaneously. The strain, however, did not affect the peak power but the peak wavelength. As the applied strain increases, the peak wavelength redshifted because the phase change of the Hi-Bi FLM with the EDF was directly proportional to the strain change. Consequently, it was possible to discriminate temperature

and strain sensitivities by using the proposed sensing method.

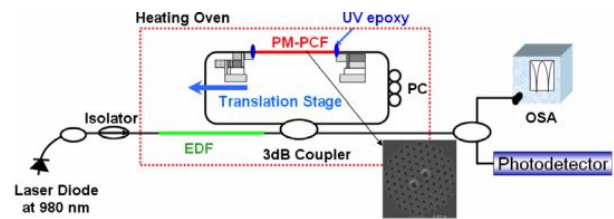


Fig. 20 Principle drawing of the system.

All the schemes proposed above have demonstrated the simultaneous measurement of temperature and strain by monitoring the certain wavelength and power of peaks. In [21], we regarded ratio of two adjacent peaks power as our demodulation result not only to decrease the influence of the unstable light power, but also double the sensitivity. This is the superiority that [22][23] don't have. Compared with the proposed schemes in section 3.1, firstly, these three schemes' demodulation results are all wavelength and power which increased the error due to the light power which is easily influenced by external environment, secondly, more optical elements are needed in these three schemes, so cost is relatively higher.

4. Conclusions

In this paper, temperature and strain characteristics of conventional and photonic crystal Hi-Bi FLM have been characterized. It is clear that cross-sensitive was the top problem when they were used as sensors. To solve this problem, Photonic crystal fiber was the best option because of its immunity to temperature. Besides, more and more simultaneous measurements of temperature and strain based on Hi-Bi FLM were proposed continually not only to avoid cross-sensitive but also provide much references to multiparameter sensor. According to different sensing principle, this letter summarized two types of methods and listed merits and demerits of each simultaneous measurement of temperature and strain. Also, there are some types of methods [24-26] which are not listed in this paper. Certainly there are some drawbacks existed in Hi-Bi FLM sensors such as: (1) it is inconvenient to apply OSA in practical engineering. (2) Hi-Bi FLM sensor only exist in laboratory because of its large scale of error. (3) The sensor production process needs to be improved. Trustfully with the research further, Hi-Bi FLM sensor will be producibility and commercialization in the near future.

Acknowledgments

Project 61074170 supported by the National Science Foundation of China. Project 090504002 and 100404006 supported by the Fundamental Research Funds for the Central Universities. Project NCET-08-0102 supported by Program for New Century Excellent Talents in University. Project 20100042110029 supported by Specialized Research Fund for the Doctoral Program of Higher Education.

References

- [1] Ping Lu, Liqiu Men, Qiying Chen.. *Applied Physics.*, **106**, 013111 1-5 (2009).
- [2] K. S. Lee, C. Shu,. *IEEE Photon Technol Lett*, **7**(12) 1444 (1995).
- [3] Y. H. Ja, *Light wave Technol*, **12**(8),1504 (1994).
- [4] A. N. Starodumov, L. A. Zenteno, D. Monzon, E. De La Rosa, *Applied Physics Letters*, **70**, 19 (1997).
- [5] D. Bo, Z. Qida, L. Feng, G. Tuan, X. Lifang, L. Shuhong, G. Hong, *Applied Optics* **45**, 7767 (2006).
- [6] H. P. Gong, *Optics Communications*, **283**, 3142 (2010)
- [7] Seunghwan Chung, Jungho Kim, Bong-Ahn Yu, ByoungHo Lee. *Ieee Photonics Technology Letters*, **13**(12), 1343 (2001).
- [8] O. Frazão, J. M. Baptista, Member, IEEE, J. L. Santos, *IEEE Sensors Journal*, **7**(10), 1453 (2007).
- [9] Y. Liu, B. Liu, X. Feng, W. Zhang, G. Zhou, S. Yuan, G. Kai, X. Dong, *Applied Optics*, **44**, 2382 (2005).
- [10] J. Noda, K. Okamoto, Y. Sasaki, *Journal of Lightwave Technology*, (4) 1071 (1986).
- [11] Orlando Frazão, José M. Baptista José L. Santos. *Sensors*, **36**(7), 2970 (2007).
- [12] Orlando Frazão. *Optical sensing with photonic crystal fibers*. *Laser & Photon. Rev.* (6), 449 (2008).
- [13] O. Frazão, *Electronics Letters*. (44) 2008.
- [14] O. Frazão. *Temperature-Independent Strain Sensor Based on a Hi-Bi Photonic Crystal Fiber Loop Mirror*. *IEEE Sensors Journal*. (7) 1453 (2007).
- [15] O. Frazão. *Applied Optics* **47**(27), 4841 (2008).
- [16] S. G. Leon-Saval, T. A. Birks. *Opt. Lett.* (30) 1629 (2005).
- [17] R. Thapa, K. Knabe. *Opt. Exp.* (14), 9576 (2006).
- [18] Da-Peng Zhou, Li Wei, Wing-Ki Liu. *Optics Communications* **281**, 4640 (2008).
- [19] O. Frazão, L. M. Marques, S. Santos, J. M. Baptista, J. L. Santos. *IEEE Photonics Technology Letters*, **18**(22), 2407 (2006).
- [20] Guoyong Sun, Dae Seung Moon, Youngjoo Chung, *IEEE Photonics Technology Letters* **19**(24), 2027 (2007).
- [21] Chun-Liu Zhao, Jiarong Zhao, Wei jin, *Optics Communications* **282**, 4077 (2009).
- [22] O. Frazão, J. L. Santos, J. M. Baptista, *IEEE Photonics Technology Letters* **19**(16), 1260 (2007).
- [23] Young-Geun Han, Youngjoo Chung, Sang Bae Lee, *Optics Communications*. **282**, 2161 (2009).
- [24] Ricardo M. André, Manuel B. Marques, Philippe Roy, Orlando Frazão, *IEEE Photonics Technology Letters*, **22**(15), 1120 (2010).
- [25] O. Frazão, S. O. Silva, J. M. Baptista, J. L. Santos, G. Statkiewicz-Barabach, W. Urbanczyk, J. Wojcik, *Applied Optics* **47**(27), 4841 (2008).
- [26] Orlando Razão, *IEEE Photonics Technology Letters*, **20**(12). 1033 (2008).

*Corresponding author: zhaoyong@ise.neu.edu.cn